

# Angewandte Chemie

Eine Zeitschrift der Gesellschaft Deutscher Chemiker

Supporting Information

© Wiley-VCH 2011

69451 Weinheim, Germany

## **Combined Cation- $\pi$ and Anion- $\pi$ Interactions for Zwitterion Recognition**

*Olivier Perraud, Vincent Robert, Heinz Gornitzka, Alexandre Martinez,\* and Jean-Pierre Dutasta\**

anie\_201106934\_sm\_miscellaneous\_information.pdf

## Supporting Information

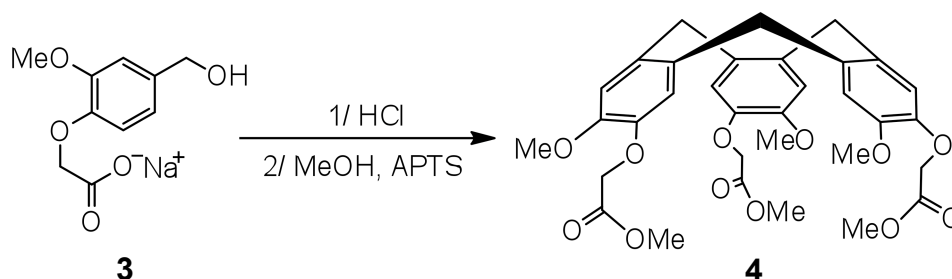
<b>Content</b>	<b>Page</b>
<b>1/ Materials and instrumentation</b>	<b>2</b>
<b>2/ Synthesis</b>	<b>2</b>
Figure S1. <sup>1</sup> H NMR spectra of compound <b>4</b>	3
Figure S2. <sup>13</sup> C NMR spectra of compound <b>4</b>	4
Figure S3. <sup>1</sup> H NMR spectra of hemicryptophane <b>1</b>	5
Figure S4. <sup>13</sup> C NMR spectra of hemicryptophane <b>1</b>	6
<b>3/ Computational methods</b>	<b>7</b>
Figure S5. Structure of the simplified models used in energy calculations.	7
<b>4/ <sup>1</sup>H NMR titrations</b>	<b>8</b>
Figure S6. Titration curve of taurine with <b>1</b>	8
Figure S7. Titration curve of homotaurine with <b>1</b>	8
Figure S8. Titration curve of GABA with <b>1</b>	9
Figure S9. Titration curve of β-alanine with <b>1</b>	9
<b>5/ Crystallographic data</b>	<b>10</b>

## 1/ Materials and instrumentation:

Compounds **3** and **5** were synthesized according to the previously reported procedure.<sup>1</sup> Solvents used were of commercial grade. <sup>1</sup>H NMR spectra were recorded at 298 K on a Bruker Avance 500 MHz spectrometer. <sup>1</sup>H NMR chemical shifts  $\delta$  are reported in ppm referenced to the protonated residual solvent signal.

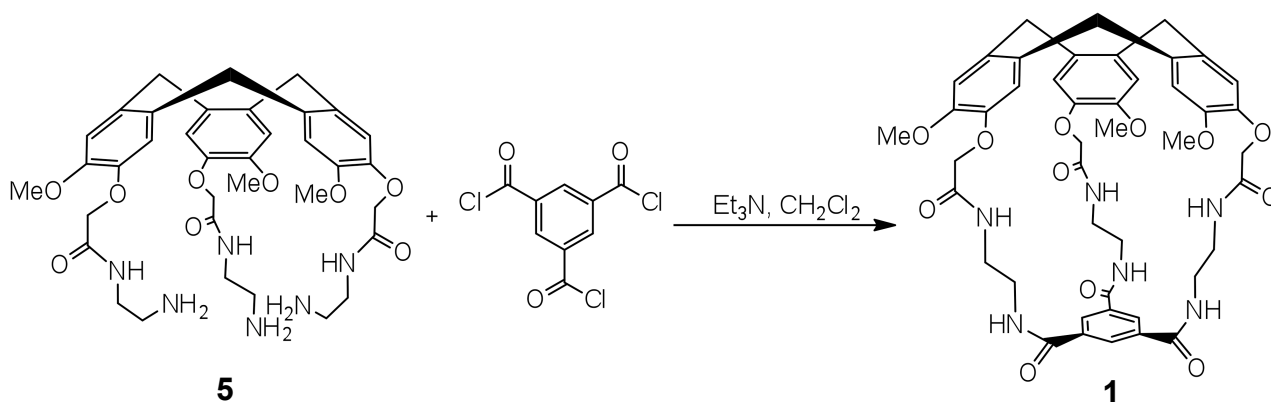
## 2/ Synthesis

### (±)-2,7,12-Tris(methoxycarbonylmethoxy)-3,8,13-trimethoxy-10,15-dihydro-5H-tribenzo[a,d,g]cyclononene (**4**)



To a solution of compound **3** (41.6 g, 0.18 mol) in water (100mL) was added 20 mL of concentrated HCl. Solvents were evaporated under reduced pressure to yield a brown oil. *p*-Toluenesulfonic acid (500 mg, 2.9 mmol) and methanol (300 mL) were added. The mixture was refluxed for 3 days and the resulting precipitate was filtered off and washed with methanol to afford **4** as a white solid (15.7 g, 42%). M.p. = 193 °C. <sup>1</sup>H NMR (CDCl<sub>3</sub>, 298 K, 497.8 MHz)  $\delta$  6.88 (s, 3H, ArH); 6.80 (s, 3H, ArH); 4.69 (d, 3H, J = 13.7 Hz, ArCH<sub>2</sub>Ar); 4.63 (d, 3H, J = 16.2 Hz, OCH<sub>2</sub>); 4.57 (d, 3H, J = 16.2 Hz, OCH<sub>2</sub>); 3.87 (s, 9H, OCH<sub>3</sub>); 3.70 (s, 9H, OCH<sub>3</sub>); 3.50 (d, 3H, J = 13.7 Hz, ArCH<sub>2</sub>Ar). <sup>13</sup>C NMR (CDCl<sub>3</sub>, 298 K, 125.2 MHz)  $\delta$  170.1 (COOMe); 148.8 (C<sub>Ar</sub>O); 146.1 (C<sub>Ar</sub>O); 134.2 (C<sub>Ar</sub>); 131.6 (C<sub>Ar</sub>); 117.8 (C<sub>Ar</sub>H); 113.9 (C<sub>Ar</sub>H); 67.5 (OCH<sub>2</sub>); 56.2 (OCH<sub>3</sub>); 52.3 (OCH<sub>3</sub>); 36.5 (ArCH<sub>2</sub>Ar). ESI-MS *m/z*: obsd 647.2087 [M+Na]<sup>+</sup> (calculated: 647.2104 for C<sub>33</sub>H<sub>36</sub>N<sub>4</sub>O<sub>12</sub>Na). IR (KBr)  $\bar{\nu}$  = 2952, 2927, 1741, 1510 cm<sup>-1</sup>.

### Hemicryptophane **1**



To a solution of compound **5** (466 mg, 0.66 mmol) and triethylamine (1 mL) in dry dichloromethane (200 mL) heated at 30 °C was slowly added over 6 days a solution of benzene-1,3,5-tricarbonyl trichloride (192 mg, 0.72 mmol) in dry dichloromethane (200 mL). The mixture was then filtered, concentrated under reduced pressure and washed with aqueous K<sub>2</sub>CO<sub>3</sub> (10%, 75 mL) and water (75 mL). Aqueous phase was extracted with dichloromethane (50 mL), combined organic layers were dried over Na<sub>2</sub>SO<sub>4</sub> and the organic

<sup>1</sup> G. Vériot, J.-P. Dutasta, G. Matouzenko, A. Collet, *Tetrahedron* **1995**, *51*, 389-400.

solvent was removed under reduced pressure to afford **1** as a white solid (124 mg, 22 %).  $^1\text{H}$  NMR ( $\text{CDCl}_3$ , 298 K, 497.8 MHz)  $\delta$  7.99 (s, 3H, ArH); 7.83 (b, 3H, NH); 7.04 (b, 3H, NH); 6.71 (s, 3H, ArH); 6.68 (s, 3H, ArH); 4.68 (d, 3H,  $J = 15.4$  Hz,  $\text{OCH}_2$ ); 4.55 (d, 3H,  $J = 13.6$  Hz,  $\text{ArCH}_2\text{Ar}$ ); 4.12 (d, 3H,  $J = 15.4$  Hz,  $\text{OCH}_2$ ); 3.93 (m, 6H,  $\text{NCH}_2$ ); 3.88 (s, 9H,  $\text{OCH}_3$ ); 3.45 (m, 6H,  $\text{NCH}_2$ ); 3.41 (d, 3H,  $J = 13.6$  Hz,  $\text{ArCH}_2\text{Ar}$ ).  $^{13}\text{C}$  NMR ( $\text{CDCl}_3$ , 298 K, 125.2 MHz)  $\delta$  170.7 (CONH); 166.9 (CONH); 148.1 ( $\text{C}_{\text{ArO}}$ ); 148.0 ( $\text{C}_{\text{ArO}}$ ); 134.0 ( $\text{C}_{\text{Ar}}$ ); 133.9 ( $\text{C}_{\text{Ar}}$ ); 133.1 ( $\text{C}_{\text{Ar}}$ ); 128.5 ( $\text{C}_{\text{ArH}}$ ); 118.6 ( $\text{C}_{\text{ArH}}$ ); 116.5 ( $\text{C}_{\text{ArH}}$ ); 71.8 ( $\text{OCH}_2$ ); 58.1 ( $\text{OCH}_3$ ); 40.1 ( $\text{NCH}_2$ ); 39.8 ( $\text{NCH}_2$ ); 35.9 ( $\text{ArCH}_2\text{Ar}$ ). ESI-MS  $m/z$ : obsd 887.3210  $[\text{M}+\text{Na}]^+$  (calculated: 887.3228 for  $\text{C}_{45}\text{H}_{48}\text{N}_6\text{O}_{12}\text{Na}$ ). IR (KBr)  $\bar{\nu} = 3378, 1656, 1523$   $\text{cm}^{-1}$ .

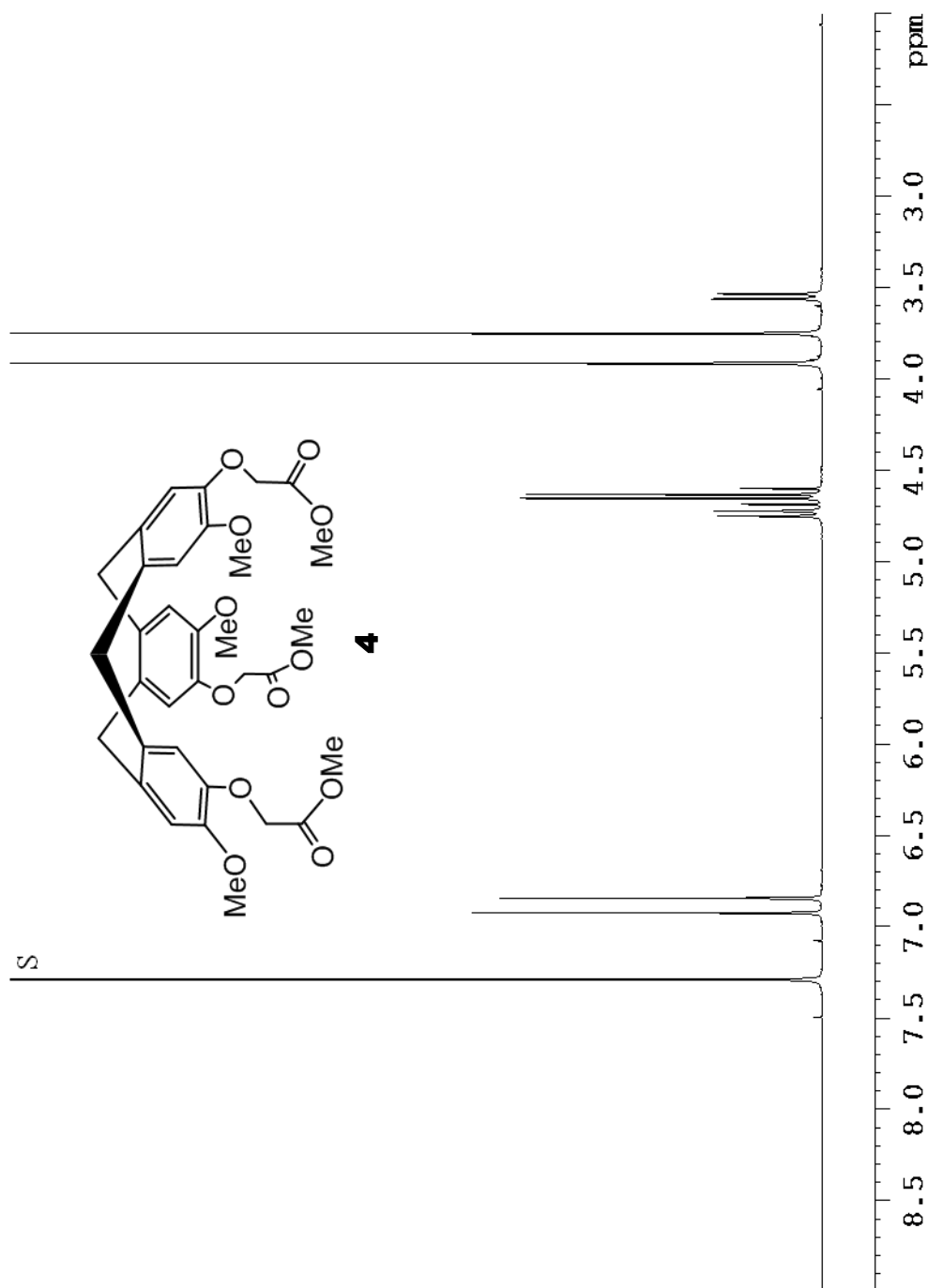


**Figure S1.**  $^1\text{H}$  NMR spectra ( $\text{CDCl}_3$ , 497.8 MHz, 298 K) of compound **4**. S: residual solvents ( $\text{CHCl}_3$ ).

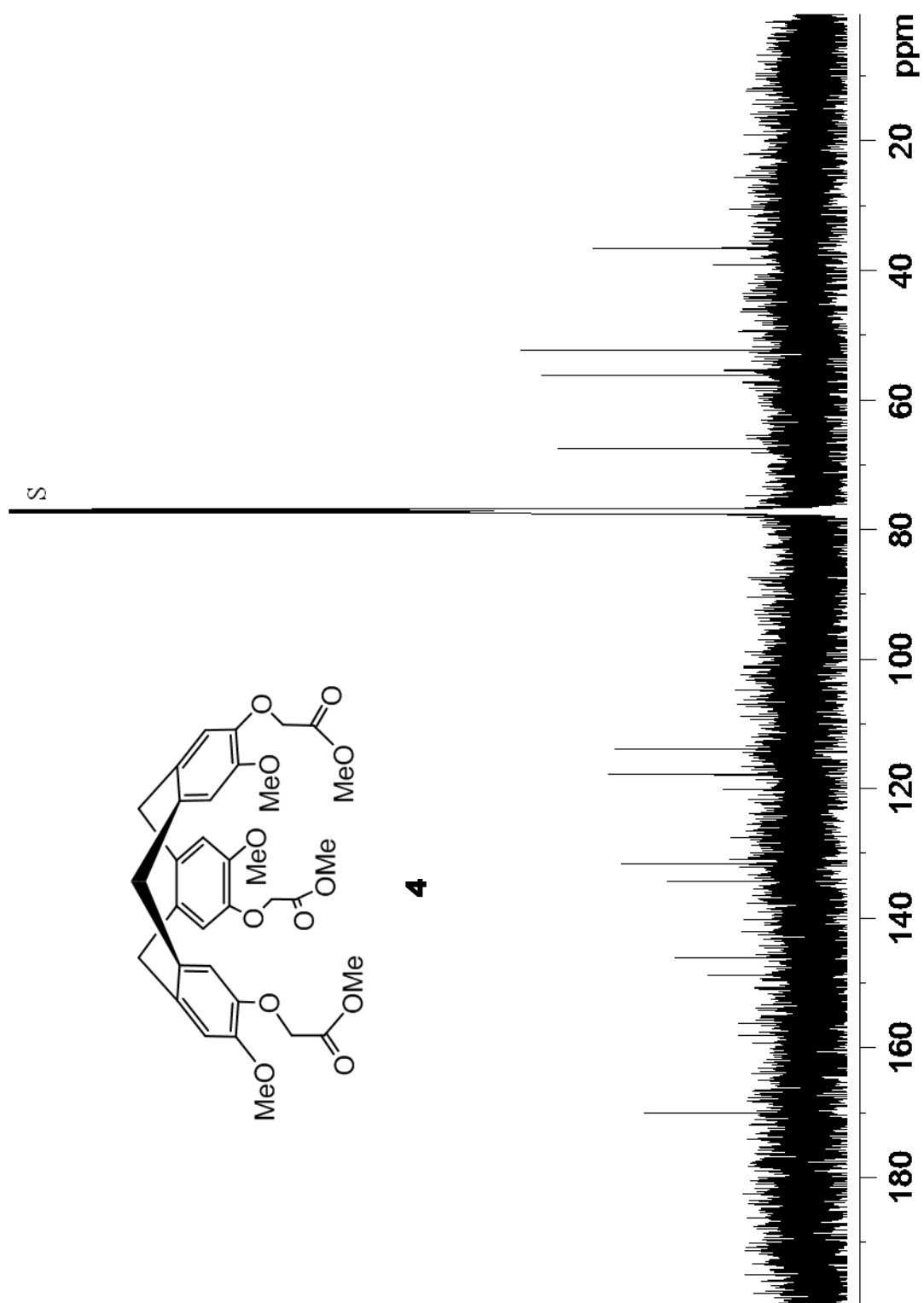


**Figure S2.**  $^{13}\text{C}$  NMR spectra ( $\text{CDCl}_3$ , 125.2 MHz, 298 K) of compound **4**. S: residual solvents ( $\text{CHCl}_3$ ).

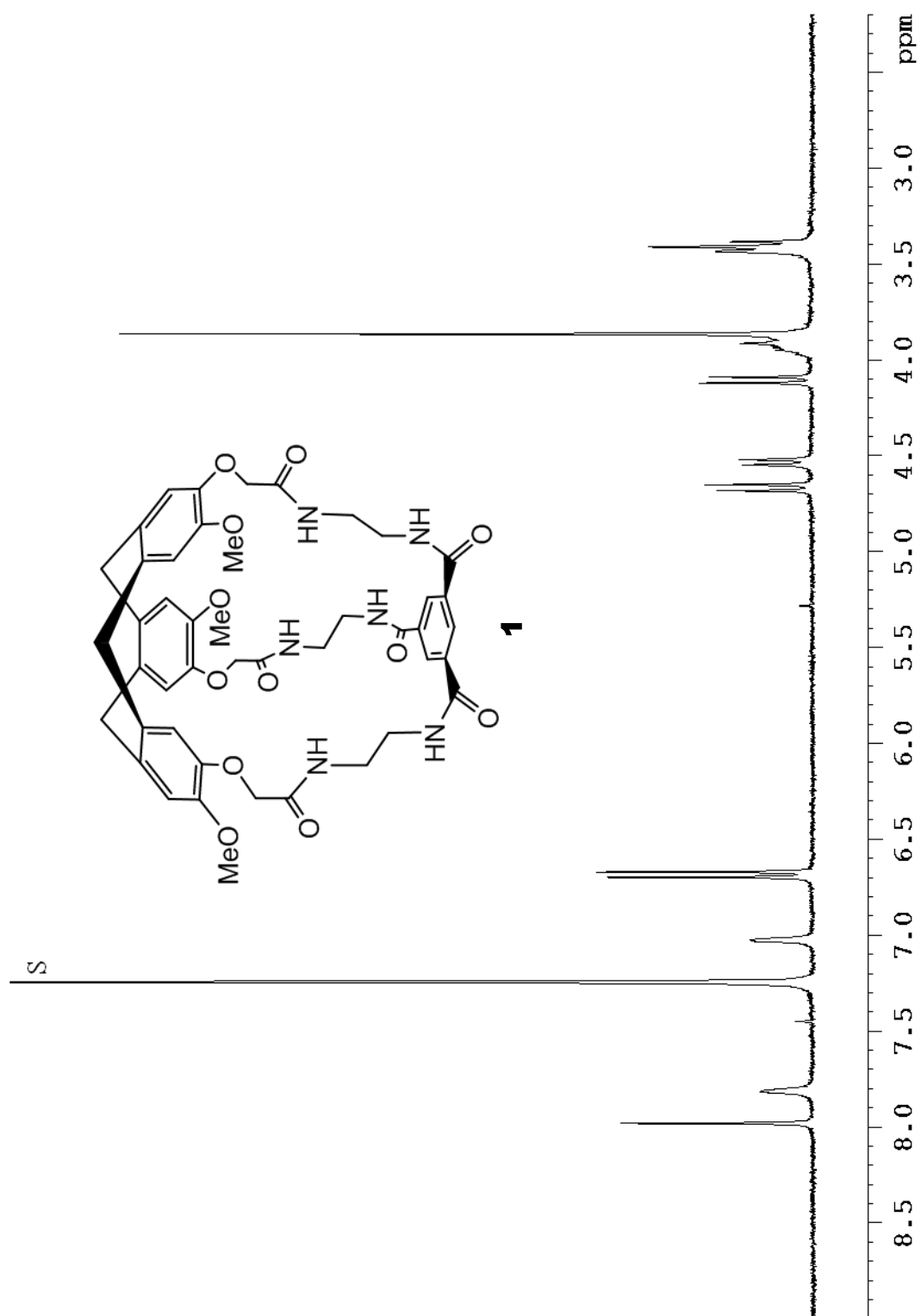


**Figure S3.** <sup>1</sup>H NMR spectra (CDCl<sub>3</sub>, 497.8 MHz, 298 K) of hemicryptophane **1**. S: residual solvents (CHCl<sub>3</sub>).

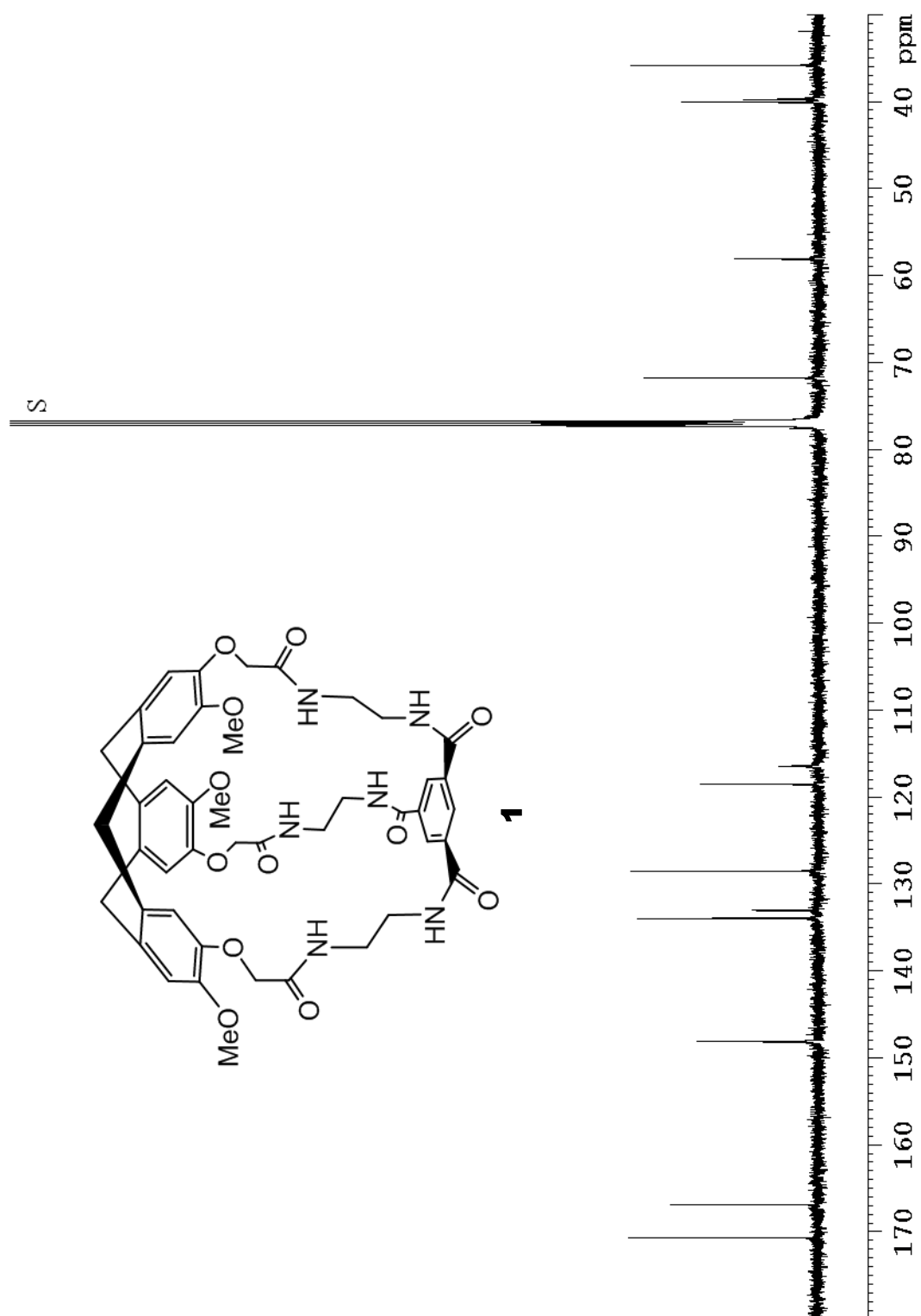


**Figure S4.**  $^{13}\text{C}$  NMR spectra ( $\text{CDCl}_3$ , 125.2 MHz, 298 K) of hemicryptophane **1**. S: residual solvents ( $\text{CHCl}_3$ ).

### 3/ Computational methods:

First, geometries determinations were performed using the Gaussian 03 package<sup>2</sup> within a restricted DFT framework. A combination of restricted BP86 functional and triple-zeta 6-311G all electron basis sets has proven to be very satisfactory for geometry optimizations. We checked using the hybrid B3LYP functional that our results do not suffer from the arbitrariness of the exchange correlation functional. The outcoming geometry was then used to further inspect the presence of cation- $\pi$  and anion- $\pi$  interactions.

Ion- $\pi$  interactions result from charge density fluctuations (*i.e.*, dispersion interactions) within a given  $\pi$  system in the presence of a static electric field produced, for instance, by point charges. Therefore, multi-reference calculations are particularly attractive since one can effectively account for this physical phenomenon, which is typically beyond a mean-field picture. In order to highlight the fluctuations within the  $\pi$  system of the aromatic ring, the expansion of the wavefunction was limited to the  $\pi$ - $\pi^*$  excitations. Considering the relatively large size of the receptor, simplified models were used for the north and south parts (see Figure S5). These models were taken from the DFT optimized structure. Complete active space self-consistent field (CASSCF) calculations were performed including 6 electrons in 6 molecular orbitals (CAS[6,6]). The CASSCF solution was converged onto the benzene-like molecular orbitals. Using this strategy, one can account for the energy contribution arising exclusively from charge density fluctuations of the  $\pi$  network with respect to the zwitterion-receptor separation  $z$ . Let us stress that the configuration interaction was limited to this particular level and no subsequent perturbative treatment was performed. The reference energies were set to zero for infinite distance separations between the zwitterion and north/south parts. Finally, assuming the additivity between the northern and southern contributions (cation- $\pi$  and anion- $\pi$ , respectively) the total ion- $\pi$  energy variations were examined as a function of  $z$ . Since our purpose was to concentrate the numerical effort on the  $\pi$ - $\pi^*$  charge fluctuations, extended basis sets were used for the aromatic ring, namely ANO-RCC triple zeta + polarization (TZP) 4s3p2d1f for C atoms while the other atoms were depicted using ANO-RCC DZP basis sets. The zwitterion atoms were depicted with ANO-RCC TZP basis sets. All our calculations were performed using the MOLCAS 7.2 suite of program.<sup>3</sup>

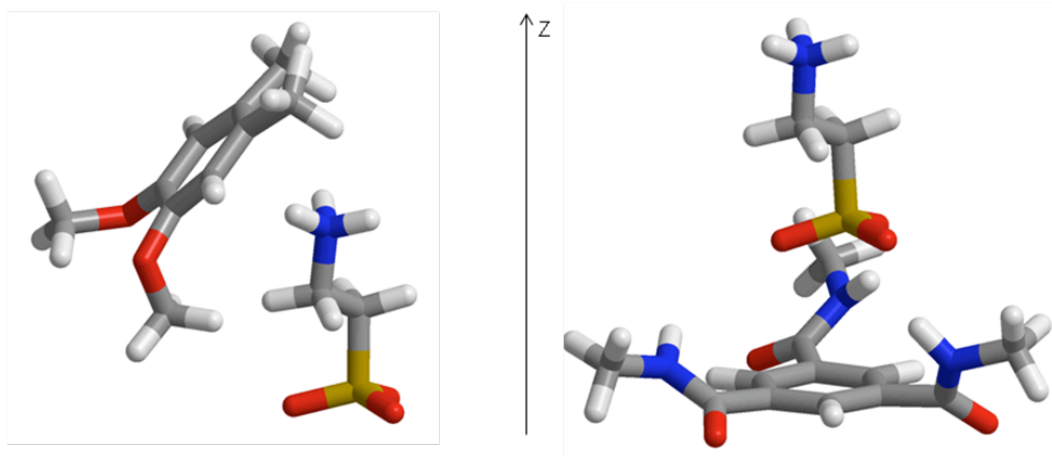


**Figure S5.** Structures of the simplified models of the north part (a) and the south part (b) of the host used to measure  $E_c$  and  $E_a$  respectively. The total ion- $\pi$  energy was calculated thanks to the relation  $E_{\text{tot}} = E_a + 3E_c$ .

<sup>2</sup>

Gaussian 03: M. J. Frisch, G. W. Trucks, H. B. Schlegel, G. E., Scuseria, M. A. Robb, J. R. Cheeseman, G. Scalmani, V. Barone, B. Mennucci, G. A. Petersson, H. Nakatsuji, M. Caricato, X. Li, H. P. Hratchian, A. F. Izmaylov, J. Bloino, G. Zheng, J. L. Sonnenberg, M. Hada, M. Ehara, K. Toyota, R. Fukuda, J. Hasegawa, M. Ishida, T. Nakajima, Y. Honda, O. Kitao, H. Nakai, T. Vreven, J. A. Montgomery, Jr., J. E. Peralta, F. Ogliaro, M. Bearpark, J. J. Heyd, E. Brothers, K. N. Kudin, V. N. Staroverov, R. Kobayashi, J. Normand, K. Raghavachari, A. Rendell, J. C. Burant, S. S. Iyengar, J. Tomasi, M. Cossi, N. Rega, J. M. Millam, M. Klene, J. E. Knox, J. B. Cross, V. Bakken, C. Adamo, J. Jaramillo, R. Gomperts, R. E. Stratmann, O. Yazyev, A. J. Austin, R. Cammi, C. Pomelli, J. W. Ochterski, R. L. Martin, K. Morokuma, V. G. Zakrzewski, G. A. Voth, P. Salvador, J. J. Dannenberg, S. Dapprich, A. D. Daniels, O. Farkas, J. B. Foresman, J. V. Ortiz, J. Cioslowski, and D. J. Fox, Gaussian, Inc., Wallingford CT, **2009**.

<sup>3</sup>

MOLCAS The Next Generation, *J. Comput. Chem.* **2010**, *31*, 224-247.



## 4/ $^1\text{H}$ NMR titrations:

A solution of guest ( $1.0 \cdot 10^{-4}$  M in a mixture  $\text{CD}_3\text{CN}/\text{D}_2\text{O}$  80/20, 500  $\mu\text{L}$ ) was titrated in NMR tubes with 10  $\mu\text{L}$  aliquots of a concentrated solution ( $5.0 \cdot 10^{-4}$  M in the same solvent) of host **1**. The shifts  $\Delta\delta$  of the guest's protons signals were measured after each addition and plotted as a function of the host/guest ratio. Association constant  $K_a$  was obtained by nonlinear least-squares fitting of these plots using WinEQNMR2 program.<sup>4</sup>

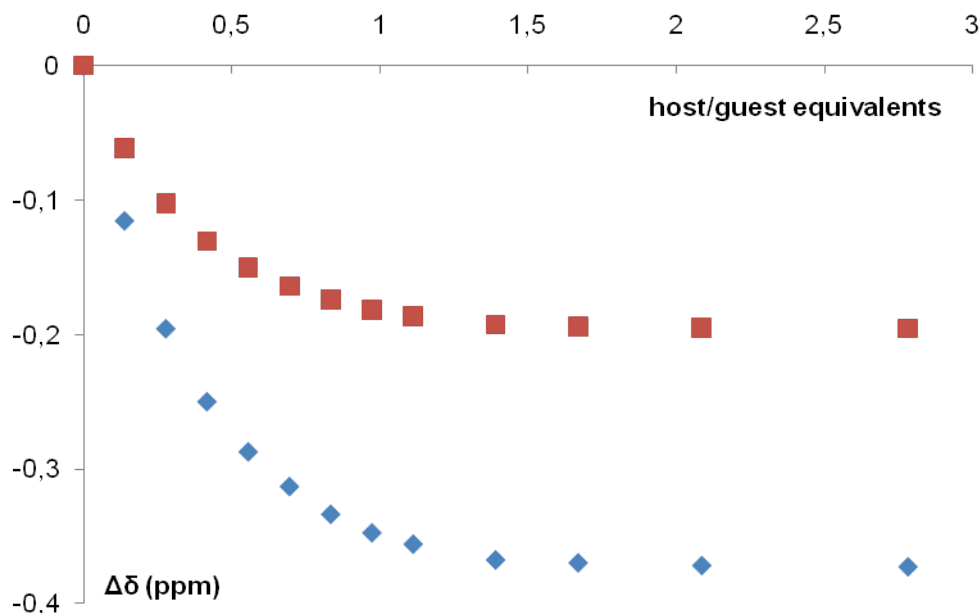


**Figure S6.** Titration curve of taurine **7** with **1**.

The chemical induced shifts  $\Delta\delta$  on taurine's protons ( $\blacklozenge$ :  $\text{NCH}_2$ ;  $\blacksquare$ :  $\text{CH}_2\text{SO}_3$ ) were measured and plotted as a function of the ratio  $[\mathbf{1}]/[\text{taurine}]$ .

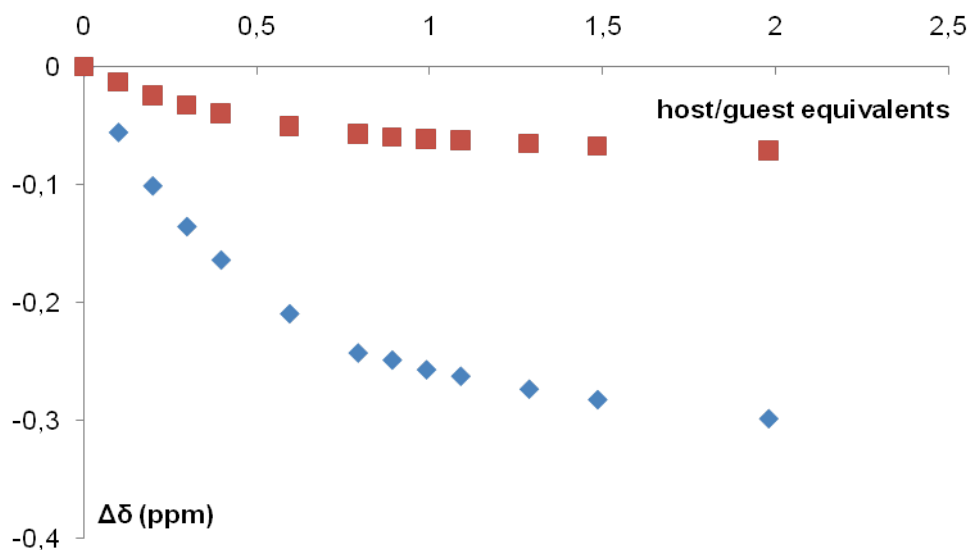


**Figure S7.** Titration curve of homotaurine **9** with **1**.

The chemical induced shifts  $\Delta\delta$  on homotaurine's protons ( $\blacklozenge$ :  $\text{NCH}_2$ ;  $\blacksquare$ :  $\text{CH}_2\text{SO}_3$ ) were measured and plotted as a function of the ratio  $[\mathbf{1}]/[\text{homotaurine}]$ .

<sup>4</sup> M. J. Hynes, *J. Chem. Soc. Dalton Trans.* **1993**, 311-312.

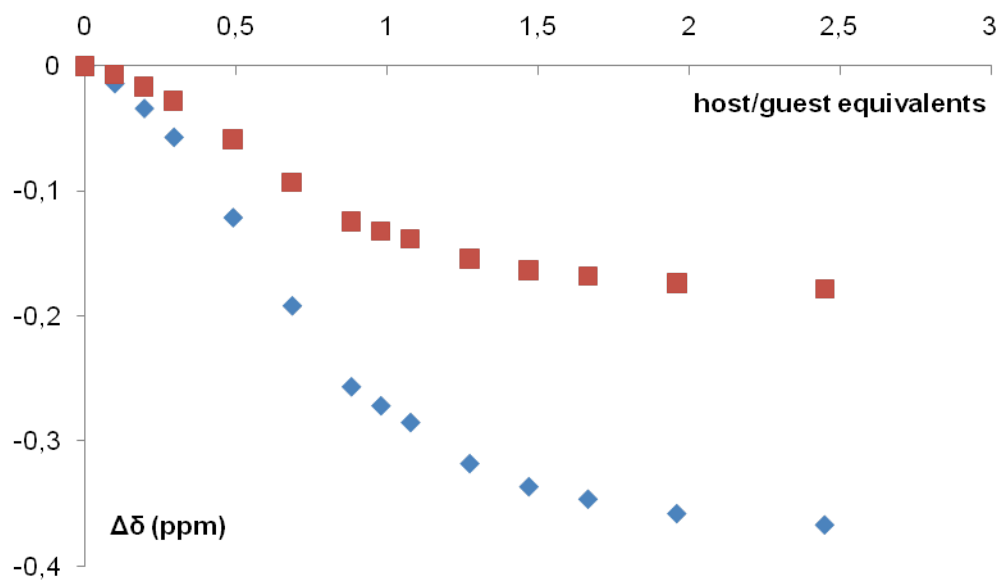


**Figure S8.** Titration curve of GABA **10** with **1**. The chemical induced shifts  $\Delta\delta$  on GABA's protons ( $\blacklozenge$ : NCH<sub>2</sub> ;  $\blacksquare$ : CH<sub>2</sub>CO<sub>2</sub>) were measured and plotted as a function of the ratio [1]/[GABA].

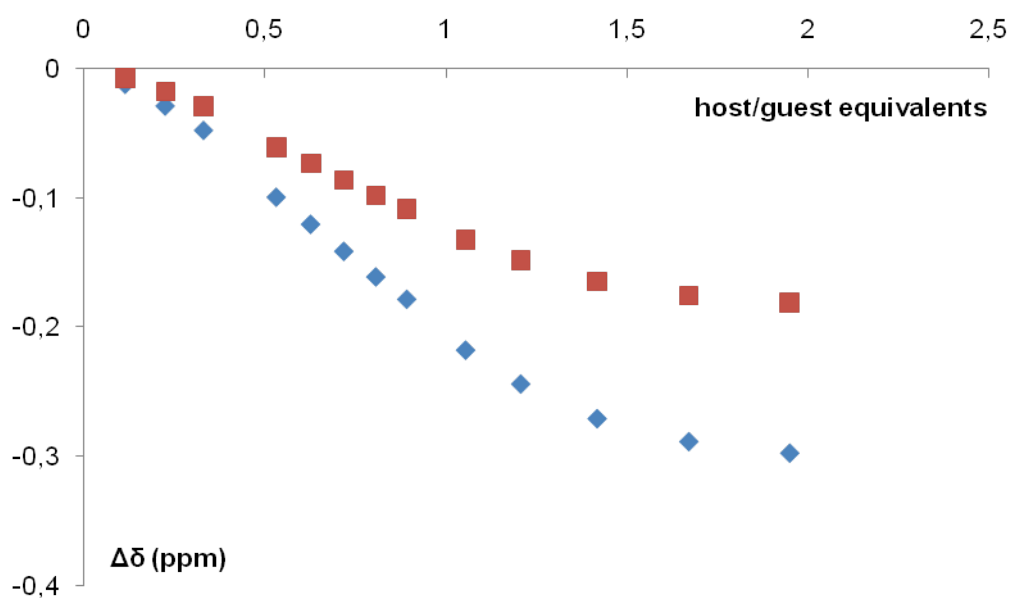


**Figure S9.** Titration curve of beta-alanine **6** with **1**. The chemical induced shifts  $\Delta\delta$  on beta-alanine's protons ( $\blacklozenge$ : NCH<sub>2</sub> ;  $\blacksquare$ : CH<sub>2</sub>CO<sub>2</sub>) were measured and plotted as a function of the ratio [1]/[beta-alanine].

## 5/ Crystallographic data

All data were collected at low temperature using an oil-coated shock-cooled crystal on a Bruker-AXS APEX II diffractometer with MoK $\alpha$  radiation ( $\lambda = 0.71073 \text{ \AA}$ ). The structure was solved by direct methods<sup>5</sup> and all non-hydrogen atoms were refined anisotropically using the least-squares method on  $F^2$ .<sup>6</sup>

**1**: C<sub>45</sub>H<sub>65</sub>N<sub>6</sub>O<sub>20.50</sub>, Mr = 1018.03, crystal size = 0.40 x 0.10 x 0.05 mm<sup>3</sup>, monoclinic, space group C2/c,  $a = 18.952(1) \text{ \AA}$ ,  $b = 13.291(1) \text{ \AA}$ ,  $c = 39.927(2) \text{ \AA}$ ,  $\beta = 91.456(2)^\circ$ ,  $V = 10053.7(7) \text{ \AA}^3$ ,  $Z = 8$ ,  $\lambda = 0.71073 \text{ \AA}$ ,  $T = 180(2) \text{ K}$ , 88780 reflections collected, 7149 unique reflections (Rint = 0.1012), R1 = 0.0689, wR2 = 0.1740 [ $I > 2\sigma(I)$ ], R1 = 0.1383, wR2 = 0.2185 (all data), residual electron density = 0.537 e  $\text{\AA}^{-3}$ .

CCDC 846246 contains the supplementary crystallographic data for **1**. These data can be obtained free of charge from The Cambridge Crystallographic Data Centre via [www.ccdc.cam.ac.uk/data\\_request/cif](http://www.ccdc.cam.ac.uk/data_request/cif).

---

<sup>5</sup> SHELXS-97, G. M. Sheldrick, *Acta Crystallogr.* **1990**, *A46*, 467-473.

<sup>6</sup> G. M. Sheldrick, *Acta Cryst.* **2008**, *A64*, 112-122.